STATE OF ILLINOIS
DEPARTMENT OF REGISTRATION AND EDUCATION

Properties of Chert Related to Its Reactivity in an Alkaline Environment

Gordon S. Fraser
Richard D. Harvey
Paul C. Heigold

ILLINOIS STATE GEOLOGICAL SURVEY
John C. Frye, Chief
Urbana, IL 61801

CIRCULAR 468
1972

Properties of Chert Related to Its Reactivity in an Alkaline Environment

Gordon S. Fraser, Richard D. Harvey, and Paul C. Heigold

ABSTRACT

Seventeen samples of chert, most of them associated with carbonate rocks, were tested for their potential reactivity in concrete. The tests determine the degree to which a sample of chert will dissolve in an alkaline solution and reduce the alkalinity of that solution. The results of the tests were correlated with the petrographic, chemical, and physical properties of the various samples.

A parabolic relation was observed between the reduction in alkalinity and the quartz content of the samples. The mean index of refraction of the samples was adjusted for X-ray crystallinity by multiple regression methods, and these adjusted values showed a linear correlation with the reduction in alkalinity and dissolved silica data. Samples strongly departing from these trends have especially high surface areas. In specific samples of chert, crystallinity, quartz content, and surface area affect the potential reactivity (the degree to which an aggregate may react in concrete). Their importance varies, depending on their relative values. High quartz content, low crystallinity, and a large surface area contribute to high reactivity in alkaline environments.

Electron microscope studies confirm the high solubility of chalcedonic silica in a sodium hydroxide solution but do not restrict high solubility to this fibrous variety of chert. Its fibrous habit was strongly evident on electron micrographs of specimens etched with sodium hydroxide.

INTRODUCTION

Many carbonate rocks used as aggregates for concrete contain minor amounts of chert, and chert is also present in many sands and gravels in Illinois south and west of the limit of the Wisconsinan glaciation. With certain unexplained exceptions, chert has deleterious effects on the durability of concrete. One such effect is the formation of "popouts," which occur in concrete when a circular crack develops around a chert pebble and a cone of concrete is dislodged. Buck (1961) showed that popouts were due to absorption of moisture by the chert and its subsequent expansion and contraction under freeze-thaw conditions. Wuerpel and Rexford (1940) stated that the absorptive capacity of chert appeared to be the best indicator of the potential durability of the concrete.

Another type of concrete failure caused by chert is of a physico-chemical nature and takes place when chert in the aggregate reacts with the alkaline solutions in the concrete and expands. The expansion cracks the concrete surface and causes eventual failure (Michaels, Volin, and Ruotsala, 1964). One criterion used to judge this property of chert is a chemical test (ASTM, 1970; ASTM designation C 289) designed to measure the reactivity of chert in an alkaline solution.

Although this test has been applied with some success, it is not entirely reliable, and departures of the actual durability of the concrete from the durability predicted by the tests have not been fully explained. We obtained varied results from C 289 tests of Ohio River and Mississippi River sands from various localities in southern Illinois, and these unpublished results appeared to be quite independent of both the abundance of the chert present in the sands and the index of refraction of the chert.

The causes for the variability in the reactivity of different chert samples in an alkaline solution are not completely understood. Because chalcedony and opal are reactive in alkaline solutions, some investigators attributed the variation in chert reactivity to the different amounts of opal and chalcedony in chert samples (Stanton, 1942; Mielenz, 1954, 1958b; and Mather, 1958). However, other workers noted that varieties of chert consisting of microcrystalline quartz containing no measurable amounts of opal and chalcedony also are reactive. They attribute the reactivity to increased surface area, due to the small crystal size or to the presence of micropores (Michaels, Volin, and Ruotsala, 1964), or to variations in the texture of the chert (Dunn and Ozol, 1962).

It is possible, however, that the amount of porosity, crystal size, and the type of silica present combine to affect the degree of reactivity. Folk and Weaver (1952) showed that chalcedony tends to be more porous than varieties of chert composed of microcrystalline quartz. Pelto (1956) showed that the areas of stress between adjacent fibers of chalcedony tend to localize reactivity. In these areas there is high porosity and lattice energy because the rows of ions of adjacent fibers are disoriented with respect to each other. Reactivity is localized because of the ability of sodium and hydroxyl ions to enter the areas of greater porosity and break the silicon-oxygen-silicon bond where lattice energy is high because of strain.

The purpose of our study was to discover and delineate properties of chert that correlate with its behavior in the ASTM C 289 test for potential reactivity of aggregate in concrete. Such information could indicate whether certain types of chert would be acceptable for concrete aggregates. Seventeen chert-rich samples of varied geologic occurrence were obtained and subjected to detailed petrographic analyses and physical and chemical tests. Statistical correlations of the results of the tests were made with the reactivity of the chert in alkaline solutions.

METHODS OF INVESTIGATION

Potential Reactivity

Early studies of the behavior of silica aggregate in mortar and concrete demonstrated conclusively that expansion was caused by reactions between certain siliceous constituents of aggregates and the sodium and potassium alkalies released during the hydration of portland cement. The ASTM chemical test was designed, therefore, to measure the readiness of the constituents of the aggregate to release alkali-soluble silica and also to determine the efficiency with which the alkalies were used during the reaction to produce alkali-silica gels capable of causing swelling or osmotic pressure when confined in the cement paste (Mielenz, Greene, and Benton, 1947; Mielenz, 1958a).

The potential reactivity of the chert samples was tested according to the procedure outlined in ASTM C 289 except that 100 to 140 U. S. mesh size (105 to 149 μ) was substituted for the 50- to 100-mesh size specified in C 289 because only a small amount of homogeneous sample material was available.

For each sample of chert, three 20-gram portions of the 100- to 140-mesh material were placed in a 1.000N sodium hydroxide solution for 24 hours at a constant temperature of 80° C. After 24 hours, the samples were removed and filtered, and the filtrate was tested to determine what reduction of alkalinity had occurred and how much silica had gone into solution. The measurements of the three subsamples were averaged to obtain test results for each sample of chert.

Refractive Index

For a given chert sample, a range of refractive indices is present. Instead of attempting to characterize a chert sample by a single index of refraction, the distribution of the indices was determined and a mean was calculated. Grains in the 105 to 149 μ range were treated with hydrochloric acid (HCl) to remove the carbonate grains that occurred in most samples and were then immersed in oils of successively lower indices of refraction until, with a count of 100 grains on a slide, all grains had a refractive index higher than the oil. With this oil index representing the lower limit, slides were prepared, portions of the sample being placed in immersion oils with refractive indices successively increased in steps of 0.004 index units. On each slide 100 grains were counted, and the number of grains with an index lower than that of the immersion oil was noted. The upper limit was fixed when all the grains on a slide had indices lower than that of the oil.

The number of grains that had a given index of refraction was determined by subtracting the number of grains with indices lower than the immersion oil from the number of grains with lower indices in the next higher oil index class. The percentages of the grains in each of these classes were calculated, and histograms and cumulative curves were prepared. Statistical moments were determined graphically and statistical parameters were calculated from formulas described by Folk (1965, p. 44-49).

Chemical and Mineralogical Composition

Analysis for carbon dioxide (CO_2) was made by HCl extraction and sorption methods, for sodium oxide and potassium oxide by flame photometry, and for water and organic carbon by gravimetric methods; the remaining elements were determined by X-ray fluorescence. From the weight percentages of the oxides, the mineralogical composition was calculated by using normative computation methods, discussed below.

The proportion of the total magnesium oxide (MgO) in the sample allocated to dolomite mineral $[MgO]_{ap,\ dol}$ was determined by computing the atomic proportion* of CO_2 exceeding that of calcium oxide (CaO). That is:

$$[MgO]_{ap,\ dol} = [CO_2]_{ap,\ spl} - [CaO]_{ap,\ spl},$$

where ap refers to the atomic proportion of the oxide, dol to dolomite, and spl to the whole sample. This computation assumes the ideal composition of dolomite ($[CaO]_{ap} = [MgO]_{ap}$). The percentage of normative dolomite in the sample is then equal to 100 $[MgO]_{ap}$ x 184.41, the molecular weight of dolomite. Next, the proportion of CaO that is allocated to calcite is calculated as

$$[CaO]_{ap,\ cal} = [CaO]_{ap,\ spl} - [MgO]_{ap,\ dol},$$

making the percentage of normative calcite in the sample equal to 100 $[CaO]_{ap,\ cal}$ x 100.09.

The quartz and clay content of the samples was calculated by normative methods with the following assumptions. The clay mineral was assumed to be illite with a silicon-aluminum ratio of 1.2, a molecular weight of 771, and 5.3 Al^{+3} ions per unit cell. These values are averages from a number of published and unpublished analyses of illite, the most common clay mineral in sedimentary rocks. The normative quartz is the silica that remains after the silica calculated for the clay has been subtracted from the total silica found in the chemical analysis.

---

* The atomic proportion of an oxide is equal to the weight percentage of the oxide, found in the sample by analysis, divided by the atomic weight of the oxide. Trivalent oxides Al_2O_3 and Fe_2O_3 were computed on the basis of one cation of alumina ($AlO_{3/2}$) and iron oxide ($FeO_{3/2}$).

Surface Area

The surface area of the chert particles was measured by the BET method (Thomas and Frost, *in press*). In the BET method, nitrogen from a flowing nitrogen-helium gas stream is adsorbed on the surface of the chert as a monomolecular layer. By measuring the amount of nitrogen then desorbed from the particles, the amount of exposed surface area can be calculated. The samples used in this determination were in the 105 to 149 μ size range and were pretreated with HCl to remove carbonate.

Density

The density of the whole sample was determined by volume displacement of xylene in a pycnometer. From these data and the normative composition of the samples, the density of the free silica was calculated in the following way. The normative weight percentages of dolomite, calcite, and clay were multiplied by their ideal densities to get the mass proportion of these three components. Subtracting the combined mass proportion of the dolomite, calcite, and clay from the density of the whole sample gives the mass proportion of free silica. This quantity is divided by the normative percentage of free silica in the sample to determine the density of the free silica.

Crystallinity

The degree of quartz crystal development in the chert samples was measured by determining the relative crystallinity of the sample by X-ray diffraction analysis. Samples were crushed to less than 44 μ, treated with HCl to remove the carbonate, and X-rayed. The five most common twin faces of quartz, $(10\bar{1}0)$, $(10\bar{1}1)$, $(11\bar{2}0)$, $(11\bar{2}1)$, and $(11\bar{2}2)$, of each sample, and also of a powder of a single quartz crystal that showed no visible twinning, were X-rayed at a scan speed of a quarter of a degree per minute.

The height (h) of the peak above the X-ray background line and the width (w) of the peak at half height were then measured, and the degree of peakedness of the diffraction pattern, or the crystallinity of the five peaks, was determined from the h/w for each peak. The crystallinity calculation of each of the five twin planes of a chert sample was divided by the crystallinity of the corresponding peaks of the reference quartz crystal and multiplied by 100 to give the index of crystallinity of the chert samples as a percentage relative to that of the reference quartz.

Petrography

Determinations of whether chalcedony or microcrystalline quartz was the type of chert present, its grain size, the type of carbonate present, and how it occurs were made by studying thin sections with a petrographic microscope. Polished, fractured, and etched surfaces of the samples were studied with a scanning electron microscope. Attention was focused on the texture of the rock, especially the pore structure and the size and shape of the grains.

TABLE 1—GEOLOGIC OCCURRENCE AND LOCATION OF SAMPLES

Sample	Petrography	Geologic unit	Location
C 60-1	Black nodular chert in fossiliferous micritic limestone	Kinkaid Limestone	Union County
C 60-3	Black lenticular chert in 1-ft bed of fossiliferous, micritic limestone	Kinkaid Limestone	Johnson County
C 60-4	Gray, nodular, cherty limestone along bedding plane	Backbone Limestone	Union County
C 60-5	Brownish gray bedded chert 1 to 5 in. thick in biomicritic limestone	Sexton Creek Formation	Alexander County
C 60-6	Gray nodular chert with calcite geodes in oolitic, foraminiferal, sparitic limestone	Fredonia Member, Ste. Genevieve Limestone	Hardin County
C 62-16	Gray lenticular chert in fossiliferous limestone	Burlington-Keokuk Limestone	McDonough County
66-85	Chert with brown and gray bands from calcarenitic dolomitic limestone	Salem Formation	Brown County
69-108 D	Nodular chert in light gray dolomite	Joliet Dolomite	Kankakee County
69-113	Dark gray nodular chert in sparsely fossiliferous micritic limestone	St. Louis Limestone	Hardin County
69-114	Chalcedony in vesicular, calcareous volcanic tuff	Kane Wash Formation	Arrow Canyon Range, Nev.
69-115	Brown radiolarian chert in beds 3 to 5 in. thick separated by thin shale partings	Franciscan Formation	San Francisco (Twin Peaks), Cal.
69-116	Brown silicified gastropods	"Gastropod limestone"	Granite County, Mont.
193-4	Calcareous, geodiferous chert in crinoidal limestone	Warsaw Formation	Adams County
215	Pinkish brown chert in calcarenitic, dolomitic limestone	Salem Limestone	Adams County
F R P	Chert with gray and brown bands in limestone (?)	Faneport Limestone	Flint Ridge Park, Ohio
M P M	White residual chert associated with barite deposit	Potosi Formation	Near Old Mines, Mo.
C 69-1	Black lenticular chert in micritic limestone	Brazil Formation	Near Veedersburg, Ind.

DESCRIPTION OF SAMPLES

Chert samples from various locations and geologic settings were collected for the study (table 1). Most of them were associated with limestones. A petrographic microscope was used to classify the samples into three groups on the basis of grain size (table 2).

Most samples were predominantly fine grained (pls. 1A and 1B) and most grains were less than 10 μ in size. Grain size varies in this group, however, and scattered patches of larger grains occur throughout the samples (pl. 1B); a few samples contain patches of fibrous chalcedony. In thin section, the samples were generally stained brown, and only the larger quartz crystals were clear. All the fine-grained samples contained some fossils, ranging from very abundant to sparse. Most of the fossils were crinoid fragments, but brachiopod and ostracod particles also were identified. All fossils showed corrosion of the margins, and many were partly or completely replaced by silica (pl. 1E). A few carbonate grains other than fossils—fine-grained anhedral calcite and scattered rhombic grains of dolomite—were observed.

Medium-grained samples predominantly measured from 10 μ to 25 μ. Grain size in these samples, too, varied, however, and many patches of larger (pl. 2D) and smaller crystals were noted. The samples were generally stained brown, and the amount of chalcedony was somewhat higher than in the fine-grained group. Fossil content of this group of samples was low, only one sample (C 69-1) showing abundant fossils in grain-to-grain contact. Most fossils in this group showed some replacement by chert, and all fossils had corroded margins. Nonfossil carbonate content also was low; very fine-grained, anhedral, sparry calcite occurred as scattered grains and dolomite as scattered rhombic crystals (pl. 2C).

The coarse-grained samples had a predominant grain size of more than 25 μ. Grains varied greatly in size, however, with small crystals occurring in irregular patches and very large quartz crystals occurring in voids (pl. 1D). Chalcedony was an abundant constituent of these samples and in some occurred as patches of very long prismatic or fibrous quartz (pl. 1C). Only one sample contained fossils, gastropods in grain-to-grain contact that were complete, unreplaced, and uncorroded specimens. Nonfossil carbonate content was high, consisting mainly of patches of very fine-grained, anhedral, sparry calcite crystals in the matrix (pl. 1F) or as subhedral crystals in the voids.

Electron Microscopy of Chert Samples

The texture of the very fine-grained material in the chert samples, observed by electron microscopy, varied from well defined granular and porous (pl. 2A), with many grains subhedral in shape, to poorly defined granular and dense (pl. 2B). In the dense, granular chert, most grains had poorly defined grain boundaries on fracture surfaces. Many nodes of "incipient" grains can be recognized, but they appeared to be fused into much larger masses that are probably amorphous.

TABLE 2—PETROGRAPHIC DESCRIPTION OF CHERT SAMPLES

Sample	SiO_2 grain size (mm)	SiO_2 condition	SiO_2 occurrence	Fossils	Nonfossil carbonate
			PREDOMINANTLY FINE GRAINED (< 0.01 mm)		
C 62-16	< 0.01	Light brown stain	Matrix	Abundant, varied assemblage of corroded and replaced fragments in grain-to-grain contact	None
	0.02	Light brown	Isolated patches		
	0.05	Clear	Isolated patches		
C 60-4	0.01	Brown stain	Matrix	Abundant, varied assemblage of corroded and replaced fragments randomly oriented and not in reciprocal contact	None
	0.25	Clear	Isolated patches		
	< 0.01	Clear	Isolated patches		
69-113	< 0.01	Brown stain	Matrix	Abundant replaced fragments not in reciprocal contact	Scattered euhedral dolomite rhombs averaging 0.05 mm
	0.03	Light brown	Scattered crystals		
	0.02	Clear	Replacing fossils		
C 60-1	< 0.01	Patchy brown stain	Matrix and replacing calcite	Abundant varied assemblage of corroded and replaced fragments in grain-to-grain contact with patchy distribution	Calcite as corroded crystals in the matrix ranging from 0.1 to 2.5 mm in size
69-115	< 0.01	Dark brown	Matrix	Abundant radiolaria not in reciprocal contact	None
	< 0.01	Clear	In radiolaria		
	0.01-0.1	Clear	In veins		
69-108 D	< 0.01	Opaque gray	Matrix	Sparse unidentified bodies corroded and replaced, arranged in elongate, curved zone	Dolomite as scattered anhedral rhombs averaging 0.01 mm
	0.25	Clear	In scattered patches		
	0.1	Clear	Surrounding patches		
	< 0.01	Brown chalcedony	Void filling		
66-85	< 0.01	Clear gray	Single area	Sparse crinoids and spines and/or spicules, entirely replaced	None
	< 0.01	Brown stain	Single area		
	< 0.01	Brown stain to opaque	Single area		
	0.01	Clear	Patches		
F R P	< 0.01	Brown	Corroded, angular fragments	Corroded and replaced crinoids and spines and/or spicules	None
	< 0.01	Light brown	Subangular fragments		

TABLE 2—PETROGRAPHIC DESCRIPTION OF CHERT SAMPLES (Continued)

Sample	SiO_2 grain size (mm)	SiO_2 condition	SiO_2 occurrence	Fossils	Nonfossil carbonate
F R P (con't)	< 0.01	Light brown chalcedony	Between void and matrix	Corroded and replaced crinoids and spines and/or spicules	None
	0.5	Clear	Void filling		
C 60-5	< 0.01	Brown stain	Matrix and replacing fossils	Sparse, varied assemblage; corroded and replaced fragments not in reciprocal contact	Calcite as corroded crystals in elongate patches, averaging 0.25 mm in size; dolomite as brown-stained euhedral crystals averaging 0.02 mm in size
	0.25	Brown stained chalcedony	Patches		
	0.01	Clear	Matrix		
			PREDOMINANTLY MEDIUM GRAINED (0.01-0.025 mm)		
C 69-1	< 0.01	Brown stain	Matrix	Abundant fossil fragments of varied assemblage in grain-to-grain contact, generally corroded and replaced	Calcite occurring as scattered patches of corroded and replaced crystals averaging 0.01 mm in size
	0.01	Dark brown stain	Scattered patches		
	0.02	Clear	Scattered patches		
215	0.01	Gray	Patches	Unidentified chert-filled bodies concentrated in patches and associated with spicules and/or spines	None
	0.05	Brown chalcedony	Patches		
	0.1	Clear chalcedony	Void filling		
C 60-6	< 0.01	Brown stain	Matrix and replacing calcite and fossils in patches	Sparse crinoids with spines and/or spicules, corroded and replaced, occurring in linear trends	Calcite occurring as corroded and replaced crystals in the matrix and scattered dolomite rhombs. Many of the latter have been dissolved out of the chert, leaving rhombic voids.
	0.025	Dark brown stain	Matrix and replacing calcite and fossils in patches		
C 60-3	< 0.01	Patchy brown stain	Matrix and replacing calcite and fossils	Sparse, varied assemblage, corroded and fragmented, scattered through matrix	Calcite occurring as corroded crystals in the matrix, ranging from 0.1 to 2.5 mm in size. Few dolomite rhombs are present.

(Concluded on page 10)

TABLE 2—PETROGRAPHIC DESCRIPTION OF CHERT SAMPLES (Concluded)

Sample	SiO_2 grain size (mm)	SiO_2 condition	SiO_2 occurrence	Fossils	Nonfossil carbonate
M P M	0.02	Brownish orange stain	Matrix	None	Dolomite occurring as euhedral rhombs scattered in the matrix and averaging 0.05 mm
	0.05-0.5	Clear	Void filling		
	0.02	Clear	Acicular crystals perpendicular to void wall		
	0.01	Brown stain	Between void and matrix		
	—	Banded chalcedony	Lining the voids		
	0.01	Light brown stain	Scattered patches		
			PREDOMINANTLY COARSE GRAINED (> 0.025 mm)		
69-114	< 0.01	Brown stain	Patches	None	Calcite occurring as abundant scattered crystals averaging 5 mm in size and slightly replaced
	0.25	Brown chalcedony	Patches		
	0.5-5	Clear chalcedony	Patches		
	0.01	Clear gray	Small patches		
	0.05-0.5	Clear	Isolated crystals		
	0.5-5	Clear	Patches of crystals		
69-116	< 0.01	Dark brown stain	Matrix	Abundant gastropods and ostracods occurring as complete, unreplaced specimens in grain-to-grain contact	Calcite occurring as slightly replaced void-filling spar averaging 2.5 mm
	< 0.01	Clear	Filling fossil interiors		
	0.05	Clear	Filling fossil		
	0.1	Light brown chalcedony	Lining fossil interiors		
	0.5	Clear	Scattered crystals		
	0.01-0.5	Clear	Interlocking grains		
	0.01	Clear	Small patches		
193-4	0.01-0.5	Clear	Interlocking grains	None	Calcite occurring as scattered euhedral crystals averaging 0.025 mm
	0.01	Clear	Small patches		

Carbonate grains occurred mainly as irregularly shaped fossil fragments in the samples, and dolomite rhombs (pl. 2C) also were present in several samples (table 2). Fracture surfaces examined in the electron microscope showed frequent rhombic void spaces, especially in sample C 60-6, which was the most weathered of all the samples studied.

Folk and Weaver (1952) indicated that under the high magnification of the electron microscope the fibrous nature of chalcedony appears to be lost. Scanning electron microscopy of chert samples in this study, however, showed the fibrous nature of chalcedony on surfaces etched by sodium hydroxide (pl. 2F). This is consistent with Pelto's hypothesis (1956) that the greatest reactivity would be found at the boundaries between adjacent fibers. Reaction with an alkaline solution would therefore tend to delineate fibers.

RESULTS OF TESTS

Potential Reactivity

The potential reactivity of the samples varied considerably (table 3). Reduction in alkalinity (R_c) ranged from 51.1 to 282.2 millimoles per liter, and dissolved silica values (S_c) ranged from 123 to 575 millimoles per liter. Plotted on an ASTM reference chart (fig. 1), these results show only one sample in the deleterious zone, eleven samples in the potentially deleterious zone, and five samples in the innocuous zone. Because the particle size range we used to derive the results of the potential reactivity was smaller than the range specified in ASTM C 289, the results can be used for only relative comparisons and do not indicate the actual potential reactivity.

Refractive Index

The mean refractive index of the samples ranged from 1. 5377 to 1. 5484 (table 3), all below the mean index of normal quartz (1.5485). Within each sample the indices showed a narrow distribution, with standard deviation values generally less than 0.75 units (1.00 unit equals a refractive index range of 0.004). Thirteen of the samples showed either a symmetrical distribution around the mean or were skewed to lower values, while four samples were skewed to higher values.

Chemical and Mineral Composition

Chemical composition varied mainly in the relative amounts of silica (SiO_2), calcium oxide (CaO), and magnesium oxide (MgO) (table 4). SiO_2 made up from 44.9 to 98.3 percent of the samples, which calculated to an equivalent range of 44.02 to 97.30 percent quartz (table 5). The abundance of CaO ranged from 0.16 to 25.4 percent and that of MgO ranged from nil to 3.74 percent. These values represented ranges of 0.5 to 36.8 percent normative calcite and

EXPLANATION OF PLATE 1

Characteristic textural features of cherts observed in transmitted and crossed polarized light.
Each sample is magnified 28 times.

A. Sample F R P showing the very fine-grained nature of the chert (quartz).

B. Sample C 60-4, showing the fine-grained nature of the chert (quartz).

C. Sample 69-114, showing fibrous chalcedonic chert.

D. Same sample as C, showing a patch of coarse-grained quartz bounded by chalcedonic chert at right-hand edge. Compare with plate 2F.

E. Sample C 62-16, showing calcitic fossil fragments (light) surrounded by very fine-grained chert (dark).

F. Sample C 60-1, showing incomplete replacement of calcite (light) by chert (dark).

$\frac{1}{2}$ mm

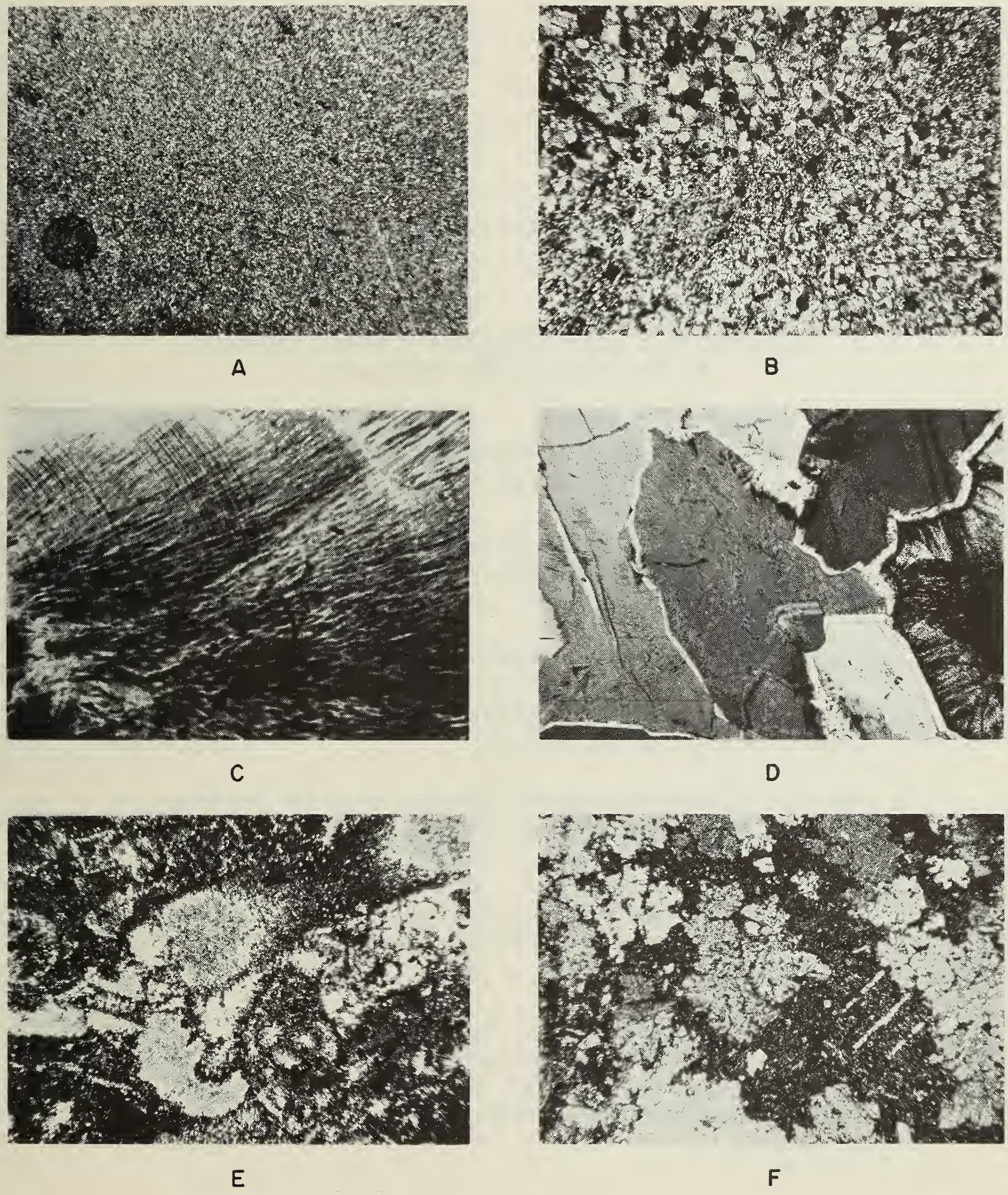

PLATE 1

Photomicrographs of chert thin sections
made with a light microscope

EXPLANATION OF PLATE 2

Characteristic textural features of cherts observed
by scanning electron microscopy.

A. Sample 69-108 D, fracture surface, showing the fine granular and porous nature of the chert (2, 000 x). └──┘ = 5 μ

B. Sample C 69-1, fracture surface, showing the poorly defined granular character of the "fine-grained" portion of the sample (11, 300 x). └──┘ = 1 μ

C. Sample C 60-3, fracture surface, showing inclusions of dolomite rhombs in dense chert. Detailed examination of this chert showed it consists of granular quartz intermediate to that shown in A and B above (600 x). └──┘ = 20 μ

D. Sample 215, fracture surface, showing one of the numerous occurrences of a patch of medium-grained quartz surrounded by finer grained quartz (2, 000 x). └──┘ = 5 μ

E. Sample C 69-1, polished and NaOH-etched surface, showing differential solution of siliceous material (10, 000 x). Compare with B above. └──┘ = 1 μ

F. Sample 66-85, polished and NaOH-etched surface, showing the contact between the relatively insoluble quartz grains (top) and soluble chalcedonic chert (bottom) (2, 000 x). This textural feature is identical to that shown at the right-hand edge of plate 1D. └──┘ = 5 μ

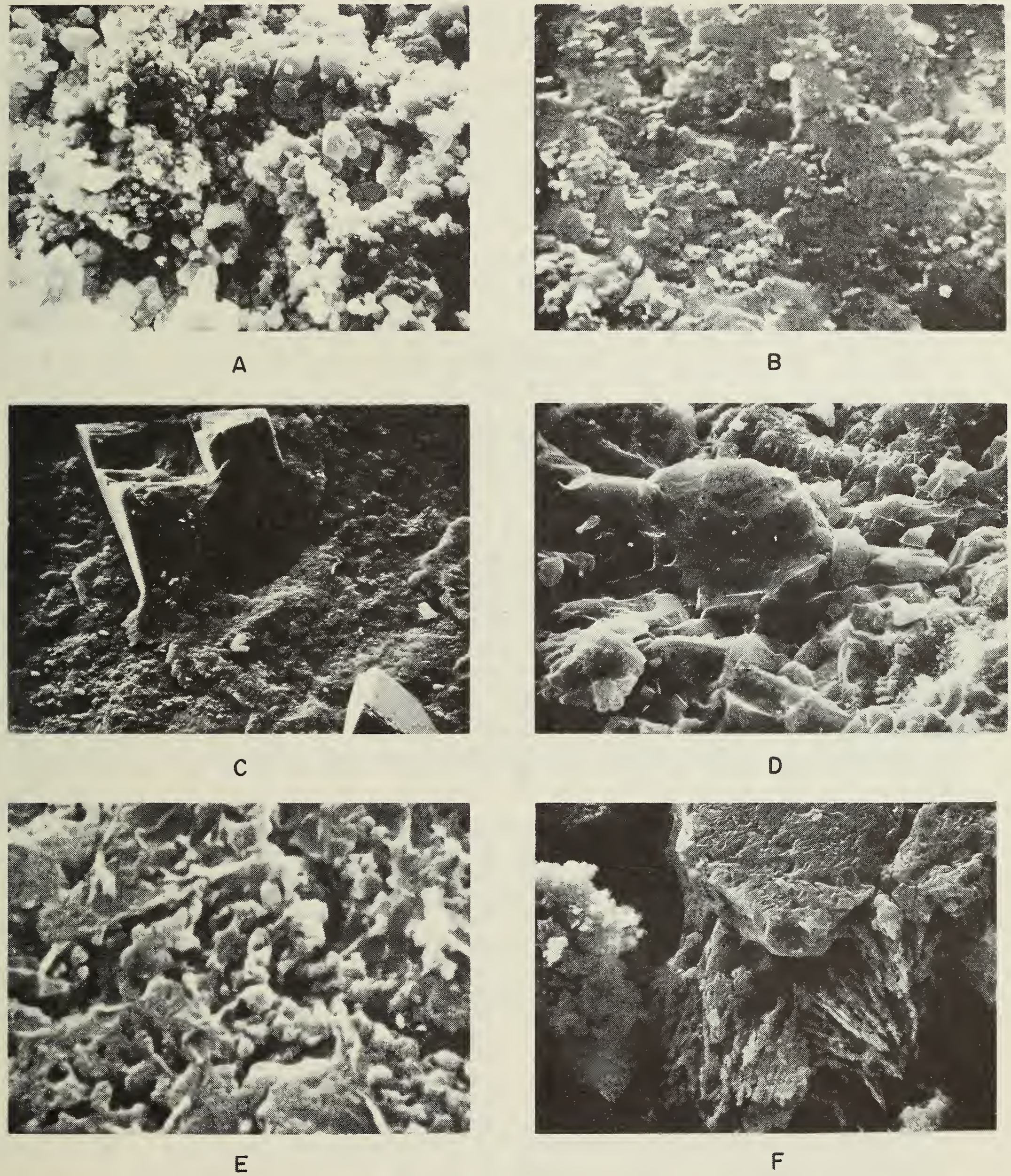

A B C D E F

PLATE 2

Photomicrographs of chert surfaces made with a scanning electron microscope

TABLE 3—RESULTS OF TESTS FOR POTENTIAL REACTIVITY

Sample	Reduction in alkalinity (R_c) (mmoles/l)	Dissolved silica* (S_c) (mmoles/l)	Mean refractive index	Refractive index skewness	Surface area* (m^2/gram)	Bulk density (g/cc)	Crystallinity index for twin planes				
							($10\bar{1}0$)	($10\bar{1}1$)	($11\bar{2}0$)	($11\bar{2}1$)	($11\bar{2}2$)
C 60-1	182.6	155	1.5414	high	3.14	2.50	85.1	61.5	36.5	53.8	26.6
C 60-3	277.1	397	1.5385	high	0.19	2.64	46.3	43.8	30.2	61.5	23.9
C 60-4	239.1	444	1.5423	symmetrical	0.43	2.57	53.7	47.5	39.7	61.5	28.4
C 60-5	222.7	415	1.5416	low	0.45	2.57	61.2	59.4	42.9	30.8	28.4
C 60-6	188.9	435	1.5428	symmetrical	2.33	2.57	59.7	48.6	42.9	69.2	32.1
C 62-16	282.2	521	1.5430	low	3.81	2.74	65.7	58.5	36.5	69.2	24.8
66-85	51.1	352	1.5465	symmetrical	0.89	2.66	100.0	83.9	66.7	92.3	56.9
69-108 D	196.2	456	1.5473	high	1.06	2.58	100.0	71.7	58.7	92.3	42.2
69-113	211.8	279	1.5377	high	0.48	2.61	92.5	71.1	84.1	61.5	22.0
69-134	250.5	575	1.5382	symmetrical	0.66	2.57	55.2	48.2	63.5	53.8	20.2
69-115	114.9	123	1.5484	high	2.33	2.81	79.1	48.6	57.1	76.9	35.8
69-116	242.5	244	1.5412	low	0.36	2.58	58.2	49.8	36.5	53.8	30.3
193-4	203.3	212	1.5402	high	0.28	2.44	88.1	61.1	69.8	69.2	100.0
215	165.1	394	1.5442	high	0.71	2.50	80.6	61.8	58.7	92.3	32.1
F R F	215.7	563	1.5385	low	1.60	2.62	52.2	47.9	52.4	53.8	23.9
M F M	145.2	410	1.5438	symmetrical	0.25	2.63	100.0	100.0	82.5	84.6	64.2
C 69-1	252.2	344	1.5396	symmetrical	1.30	—	55.1	52.1	39.7	69.2	35.8

* Analyses determined by the Chemical Group of the Illinois State Geological Survey.

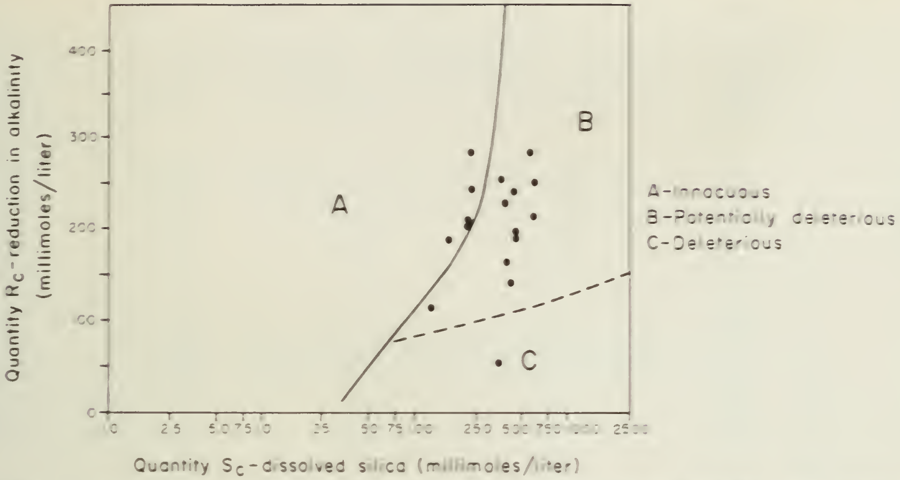

Fig. 1 - Results of tests for potential reactivity plotted on ASTM C 289 chart. Distribution of datum points in the three zones is shown, with only one sample plotted in the deleterious zone.

0.00 to 15.67 percent normative dolomite. The alumina (Al_2O_3) content ranged from nil to 2.00 percent, which corresponded to a range of 0.00 to 5.80 percent normative clay. The presence and relative abundance of the mineral constituents calculated by the normative analyses were verified by X-ray diffraction analysis and microscope study. (X-ray diffraction results show the crystalline silica in the samples occurs in the form of alpha quartz, with a minor amount of aluminum-silicate clay in some samples. No opaline silica or cristobalite was observed optically or with X-ray). Sample C 60-4, a cherty limestone, contains the least quartz (44 percent) and the highest carbonate content (52 percent) of all the samples.

Surface Area and Density

Surface area of the samples ranged from 0.19 to 3.81 square meters per gram (table 3) and averaged 1.19. Of the 17 samples, four had surface areas at least twice that of the average for all samples and six had surface areas half that of the average. The predominantly coarse-grained cherts, as determined petrographically, averaged 0.43, medium-grained samples averaged 1.15, and fine-grained samples averaged 1.38 m^2/gram.

Two of the 17 samples had calculated silica densities greater than the measured density of quartz. The remaining 15 samples ranged in density from 2.50 to 2.66 g/cm^3. Considerable error is inherent in calculating the density of silica in a sample from the density of the whole sample. The greatest error probably occurs in assuming an ideal density for dolomite and clay, which can vary considerably in density with composition.

X-ray Diffraction

The X-ray diffraction patterns of the cherts showed a slight broadening of the peaks and a decrease in intensity, but no shift in peak position was noted.

TABLE 4—CHEMICAL COMPOSITION IN WEIGHT PERCENTAGE*

(Analyses by Analytical Chemistry Section, Illinois State Geological Survey)

Sample	SiO_2	TiO_2	Al_2O_3	Fe_2O_3	MnO	MgO	CaO	Na_2O	K_2O	H_2O + (110°)	CO_2	Organic carbon
C 60-1	53.4	nil	0.27	0.52	nil	0.53	24.50	nil	0.03	0.11	20.17	0.30
C 60-3	86.0	0.01	0.06	1.51	0.03	0.05	6.30	nil	0.03	0.14	5.59	0.31
C 60-4	44.9	nil	0.12	0.71	0.02	3.74	25.40	0.07	0.07	0.26	23.67	0.08
C 60-5	82.9	nil	0.54	1.08	0.02	nil	8.12	0.11	0.13	0.41	6.62	0.46
C 60-6	91.8	0.06	1.76	0.89	0.01	0.28	1.76	0.10	0.33	0.82	0.95	0.32
C 62-16	73.6	nil	nil	0.46	0.02	0.02	13.70	0.45	0.01	0.95	10.02	0.39
66-85	98.3	0.02	0.19	0.86	0.03	0.05	0.16	0.09	trace	0.19	0.03	0.27
69-108 D	96.0	0.01	0.32	0.31	0.02	0.31	1.05	nil	0.05	nil	1.25	0.36
69-113	81.5	nil	0.40	1.51	0.03	2.79	6.01	nil	0.08	0.34	7.49	0.17
69-114	61.3	nil	0.65	1.02	0.02	0.31	19.70	nil	0.14	0.54	15.25	0.27
69-115	92.0	0.09	2.00	2.08	0.01	0.32	0.63	nil	0.41	0.70	0.46	0.15
69-116	72.6	nil	0.65	1.64	0.02	0.43	13.10	0.09	0.17	0.58	10.11	0.25
193-4	74.9	nil	0.09	0.99	0.03	0.16	12.40	0.09	0.03	nil	9.85	0.78
215	90.8	0.03	0.35	1.25	0.04	0.05	3.14	0.09	0.10	0.14	2.63	0.16
F R P	92.9	0.02	0.37	2.24	0.04	0.16	2.28	0.21	nil	0.21	1.95	0.12
M P M	94.0	nil	0.02	1.04	0.04	0.49	2.06	nil	nil	nil	2.27	nil
C 69-1	72.8	nil	0.12	0.65	0.01	nil	14.20	nil	0.02	nil	10.71	1.07

---

* Strontium occurs in each sample from trace to 0.04%. P_2O_5 is nil in 69-108 D, M P M, and 66-85 and is present from trace to 0.11% in the other samples. Other elements were not determined.

TABLE 5—MINERAL (NORMATIVE) COMPOSITION OF SAMPLES
(in percent)

Sample	Quartz	Calcite	Dolomite	Clay	Total
C 60-1	52.73	40.8	4.61	1.45	99.59
C 60-3	84.08	9.7	2.76	4.35	100.89
C 60-4	44.02	36.8	15.67	2.03	98.52
C 60-5	81.38	14.0	0.00	3.05	99.35
C 60-6	90.69	3.1	0.92	2.46	96.25
C 62-16	73.21	24.4	0.56	0.00	98.17
66-85	97.30	0.5	0.00	2.47	99.82
69-108 D	95.68	1.0	1.66	0.87	99.21
69-113	79.52	4.2	11.98	4.35	100.05
69-114	59.82	35.1	0.00	2.90	97.82
69-115	89.01	1.1	0.00	5.80	95.91
69-116	70.39	23.4	0.00	4.64	98.43
193-4	73.69	21.8	0.55	2.76	98.80
215	89.89	5.2	0.74	3.63	99.46
F R P	89.91	3.8	0.55	6.38	100.64
M P M	92.85	2.2	2.77	4.35	102.17
C 69-1	71.71	25.3	0.00	1.89	98.90

As no shift to larger d-spacings was observed in the samples in comparison with the reference crystal, common impurities in quartz such as lithium, sodium, and aluminum (Frondel, 1962) are not present in significant amounts in the quartz grains in the chert samples.

Broadening of X-ray peaks may be caused by decreasing grain size, stacking faults in the crystal structure, and variations in the lattice parameters caused by strain. Decreasing grain size causes a decrease in peak intensity in addition to broadening, so that the area under the peak remains constant (Azaroff and Buerger, 1958). Broadening is not accompanied, however, by a shift in the position of the peak.

Where broadening is due to stacking faults in the crystal structure the intensity of the peaks may be decreased, but there will be no relative shift in the peak position (Gross and Paterson, 1965). In addition, a characteristic asymmetry will develop in which the intensity of the peak will decline very gradually on the larger d-spacing side of the peak maximum.

A broadening of the peak and a decrease in intensity, along with a shift in the peak position, will result when strain has produced lattice disorder in crystals. Increased stress may be relieved by twinning or lattice dislocation (Klassen-Neklyudova, 1964). In the latter case, powder diffraction patterns will be similar to those of crystalline quartz. On the other hand, increased strain without twinning will result in increased broadening and decreased intensity of the diffraction peak and an increased shift of the peak position.

The broadened X-ray diffraction maxima of the cherts in this study are believed to be caused by an abundance of crystallites of submicron size. Although petrographic (optical) observations do not support this conclusion because most observed grains are larger than 2 μ, dislocations of the crystal lattice within grains could form subgrains of crystallites to produce the broadened X-ray maxima (W. F. Bradley, *personal communication,* 1971). Furthermore, the lattice dislocations were probably caused by strain during crystallization of the chert constituents.

NUMERICAL ANALYSIS OF RESULTS

General Statement

The petrographic, physical, and chemical tests essentially measured four properties of the chert samples: crystallinity, composition, BET surface area, and potential reactivity. The crystallinity of the chert was directly measured by the mean refractive index. Chemical composition was given by the oxide percentages, and mineral composition by the percentages of normative quartz, calcite, dolomite, and clay. Surface area indicated the amount of chert (HCl-insoluble matter) exposed to the alkaline solutions for reaction.

The results of the potential reactivity test of the chert in an alkaline environment were the dependent variables, and the crystallinity, composition, and surface area were the independent variables in subsequent correlation analyses. Linear regression analyses (table 6) of these parameters revealed no significant single petrographic property that could be used to predict the reactivity of all the samples tested. The regression analysis, however, did indicate which single variable for each property most accurately reflected the performance of the chert in the test for potential reactivity.

Multiple correlation analysis of the data was accomplished with the aid of a SOUPAC program run on the IBM 360/75 digital computer at the University of Illinois. Of particular interest in the output of this program was the correlation matrix, standardized and unstandardized regression coefficients (along with the intercept value), and the multiple correlation coefficient. The correlation matrix provides the coefficient of correlation of each variable with all other

TABLE 6—COEFFICIENTS OF CORRELATION FOR SELECTED PROPERTIES OF CHERT WITH REACTIVITY POTENTIAL

	Mean refractive index	Adjusted mean refractive index	Normative quartz (%)	Surface area
Alkali reduction	0.57	0.64	0.09	0.05
Dissolved silica	0.21	0.31	0.09	0.05

variables. The standardized regression coefficients give an assessment of the relative weights of the independent variables in contributing to the dependent variables. The unstandardized regression coefficients and the intercept value define the regression plane to be used in estimating the dependent variables. The multiple correlation coefficient is a measure of the agreement of the data with the regression plane.

The normative quartz was found to be the most important constituent affecting R_C and S_C. Of all the independent variables, the mean refractive index showed the highest correlation coefficient (0.57) with R_C. It was felt, however, that a better correlation might result if a more accurate estimate of the mean could be made, since the range of the refractive index class intervals for a given sample was high compared to the number of class intervals used to give the graphical estimate of the mean. The mean refractive index was adjusted, therefore, by using the index of crystallinity.

Determination of the Adjusted Mean Refractive Index

For multiple correlation analysis the mean refractive index of each of the samples was the dependent variable, and the indices of crystallinity of the five twin faces of a given sample were the independent variables.

The multiple correlation coefficient was calculated as 0.77, and the standardized regression coefficients showed that the first and fourth indices of crystallinity contributed most heavily to the mean refractive index. The adjusted mean refractive index of each sample was calculated from the regression plane defined by the unstandardized regression coefficients and the intercept value.

INTERRELATION OF PROPERTIES

The plots of R_C against surface area show no linear relation (cor coef 0.05), and no direct dependence of the reactivity was observed on the surface area data.

The correlation coefficient of dissolved silica and the adjusted mean refractive index was 0.31 (table 6), a poor correlation. A linear trend, however, was made evident by graphical analysis (fig. 2). The linear correlation of dissolved silica with normative quartz and surface area also was very poor, with correlation coefficients of 0.09 and 0.05, respectively (table 6), and graphical analysis indicated no nonlinear correlation.

The correlation coefficient of R_C and the adjusted mean refractive index was 0.64 (table 6), indicating that if the chert samples are normally distributed and unbiased about 32 percent of the variation of the reduction can be explained by linear dependence on the adjusted mean refractive index. Graphs of R_C against surface area show no linear relation (cor coef 0.05) and no direct dependence of the reactivity was observed in the surface area data.

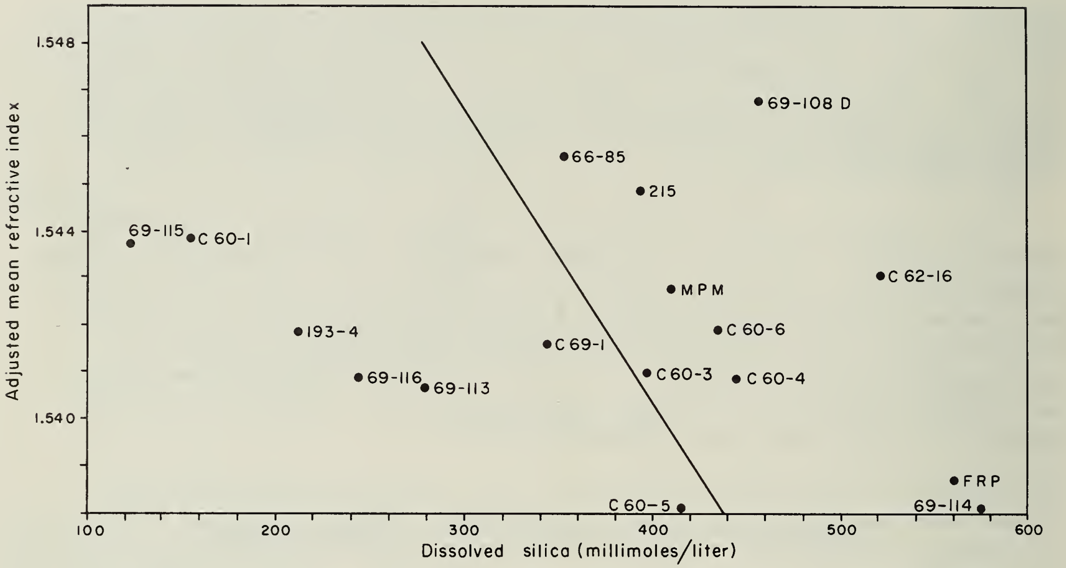

Fig. 2 - Plot of dissolved silica as a function of adjusted mean refractive index showing computer-calculated regression line.

The relation of R_C with normative quartz was found to be nonlinear and best described by a parabolic curve (fig. 3). To verify that this parabolic relation actually represented the reaction of the samples in the alkaline solution, a series of independent tests was made. The potential reactivity of a mixture of tripoli, a porous form of microcrystalline quartz, and varying amounts of calcium carbonate was determined by the ASTM C 289 test. The trend of the data from this experiment also was parabolic, closely fitting the previous curve.

The maximum R_C was reached by the chert samples at about 65 percent quartz and decreased rapidly with both increasing and decreasing amounts of quartz (fig. 3). Up to 65 percent the increasing amounts of quartz increase the R_C, as would be expected, but more than 65 percent quartz decreased the R_C. In the microcrystalline silica experiments, the same pattern emerged.

Mielenz, Greene, and Benton (1947) noted that dolomite ($CaMg(CO_3)_2$) increased the R_C by the precipitation of secondary magnesium hydroxides. This effect would reduce the concentration of hydroxyl ions in solution but would not prevent alkali ions of sodium and potassium from combining with silicates to form deleterious alkali-silica gels.

Dunn and Ozol (1962) indicated that the presence of dolomite in silica aggregates causes an increase in the R_C and a decrease in the amount of silica in solution. They ascribed the increased R_C to the formation of insoluble magnesium hydroxide. The decrease in S_C was attributed to three factors: minimization of the dissolution of silica due to the increased R_C; the presence of protective films

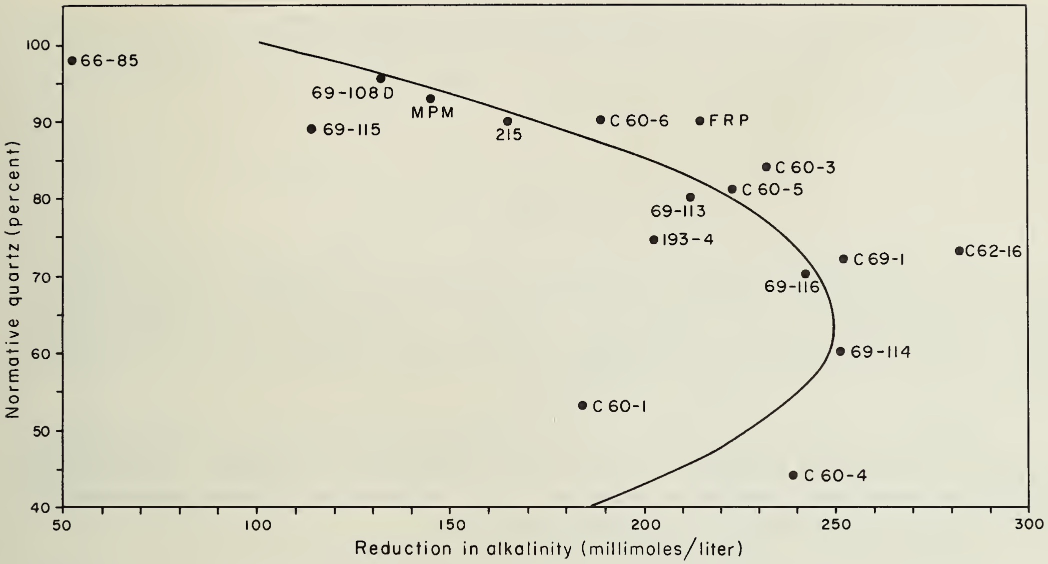

Fig. 3 - Plot of alkali reduction as a function of normative quartz showing a parabolic relation.

of magnesium hydroxide or calcium carbonate on the silica grains; and a reaction that produced insoluble silicates. Mielenz and Benton (1958) concluded that the calcium released into an alkaline solution combined with dissolved silica to form calcium silicates carrying adsorbed sodium. This would reduce the concentration of alkali ions and hydroxyl ions and decrease the amount of dissolved silica.

The reduction in the concentration of dissolved silica might also simply be due to the decreased amount of silica available for reaction as the amount of carbonate in the sample increases.

An increase in R_C without a decrease in S_C would cause an upward shift in datum points in figure 1. Datum points in the deleterious or potentially deleterious zones might be shifted upward into the innocuous zones by the addition of calcite or dolomite to the sample. If the increase in R_C is due to precipitation of insoluble calcium and magnesium hydroxides, the test result might indicate that a material is innocuous even though sodium is still available to form deleterious alkali-silica gels.

An increase in R_C with a decrease in S_C would cause a shift in datum points upward and to the left in figure 1 if calcite or dolomite were added to the sample. The shift would result following a decrease in the concentration of alkali and hydroxyl ions and in the amount of dissolved silica, as was indicated by Mielenz and Benton (1958) and Dunn and Ozol (1962). Under such conditions a point in the deleterious or potentially deleterious zones might be shifted into the innocuous zone. If, however, similar reactions occurred in concrete, the potential of the silicate-carbonate mixture to become deleterious would be reduced as the calcium silicate and absorbed alkali ions are removed, rendering them unavailable to form expandable alkali-silica gels.

Because of the spurious effects introduced by the presence of carbonates in test samples, Mielenz and Benton (1958) recommended testing reacted solutions for sodium and potassium concentration rather than for titratable hydroxyl ion concentration.

Multiple Regression Analysis

As it was apparent that no single property of a chert sample determined its potential reactivity, multiple regression analysis was used to determine the relative contributions of the properties of chert to its behavior in an alkaline solution. Because the correlation of total surface area to both R_c and S_c was poor, this property was disregarded in the analysis.

With R_c as the dependent variable and the percentage of normative quartz and the adjusted mean refractive index as the independent variables, the multiple correlation coefficient was calculated as 0.68. With S_c as the dependent variable, the multiple correlation coefficient was 0.39.

The poor linear correlation of S_c with the independent variables indicates that the relative input of refractive index and normative quartz varies considerably from sample to sample. In addition, we noted that in a few cases where one of the independent variables of a sample correlated well with R_c, the correlation with S_c was poor.

Normalization of Data Through Graphic Projection

An attempt was made to normalize the data graphically to determine the relative input of the independent variables to the potential reactivity of the individual samples. Underlying the use of the normalization procedure is the assumption that all the samples react in the same manner when one physical characteristic is allowed to vary while the others remain constant. The mathematical model used to describe this is a family of curves, each of which passes through a datum point of a particular sample. Each curve is congruent to the curve that represents the least-squares fit to all datum points by a polynomial. Each curve is oriented to the y-axis in the same way as the least-squares curve. Thus, each member of the family of curves describes the behavior of the sample as one particular characteristic is allowed to vary.

Each sample was first normalized to a composition of 100 percent normative quartz. The parabola relating R_c with the percentage of normative quartz (fig. 3) was shifted along the x-axis until a datum point intercepted the curve. The curve was then followed from that point to the point where the curve intercepted the line representing 100 percent quartz. This intercept indicated the amount of alkali reduction that would have occurred had the sample been composed entirely of quartz.

The normalized reduction in alkalinity was then plotted against the adjusted mean refractive index. Figure 4 shows a trend in contrast to the highly

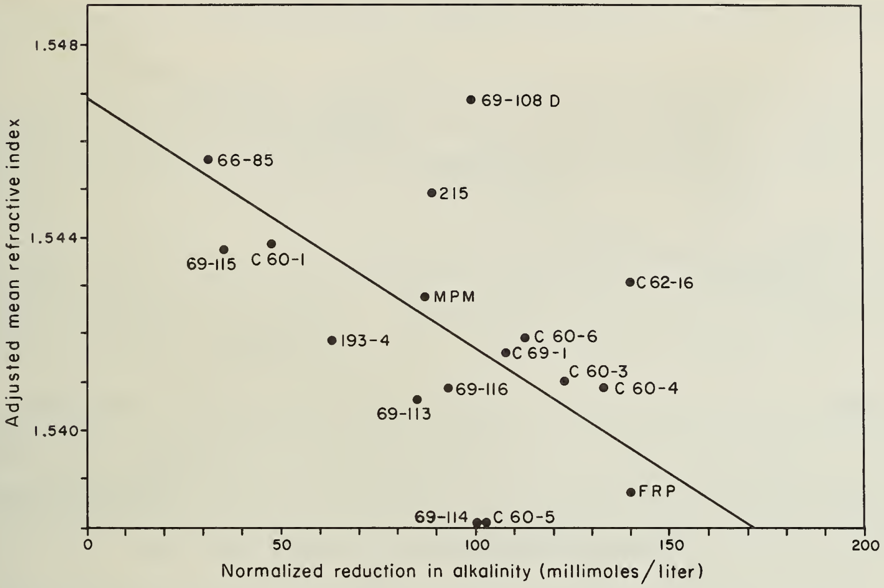

Fig. 4 - Plot of normalized alkali reduction as a function of adjusted mean refractive index.

scattered distribution of points when the adjusted mean refractive index was plotted as a function of raw R_C data.

The order of normalization was then reversed. Datum points representing R_C plotted as a function of the adjusted mean refractive index were projected parallel to the regression line calculated for this relation up to the line representing the refractive index of quartz averaged between the ϵ and ω indices (1.5485). The value indicated at the point of intersection represented the degree of reduction in alkalinity normalized to the amount the sample would have produced had it been composed of well crystallized quartz. The resulting normalized R_C was then plotted as a function of the percentage of normative quartz. This graph also showed a linear trend.

Most points fell along the trends established by both sets of projections, and these points are interpreted as representing samples in which the normative quartz and adjusted mean refractive index had an approximately equal effect on the degree of R_C. Two groups of points, however, failed to align along both trends.

The first of these groups consists of points falling along either one or the other of the trends. Three datum points fell along the second trend only and showed a high degree of departure from the first trend. These points are interpreted as representing samples in which the normative quartz played a secondary role in determining the degree of R_C for that sample. In such samples the amount of variation of the sample from the parabola relating percentage of normative quartz to R_C would have been independent of the amount of quartz present. The normalization process would then give spurious results and the datum point would

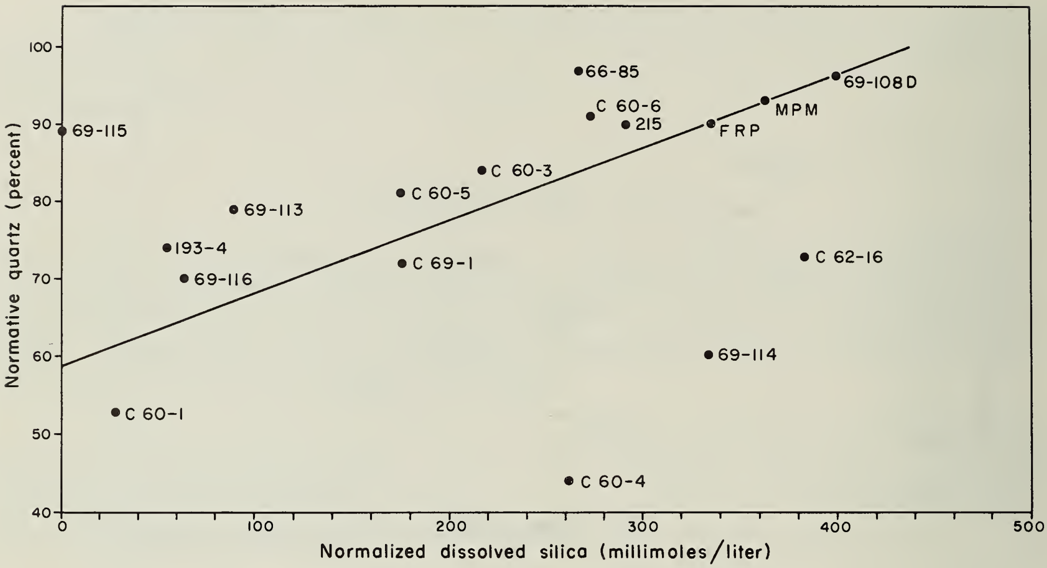

Fig. 5 - Plot of normalized dissolved silica as a function of normative quartz showing well defined linear trend.

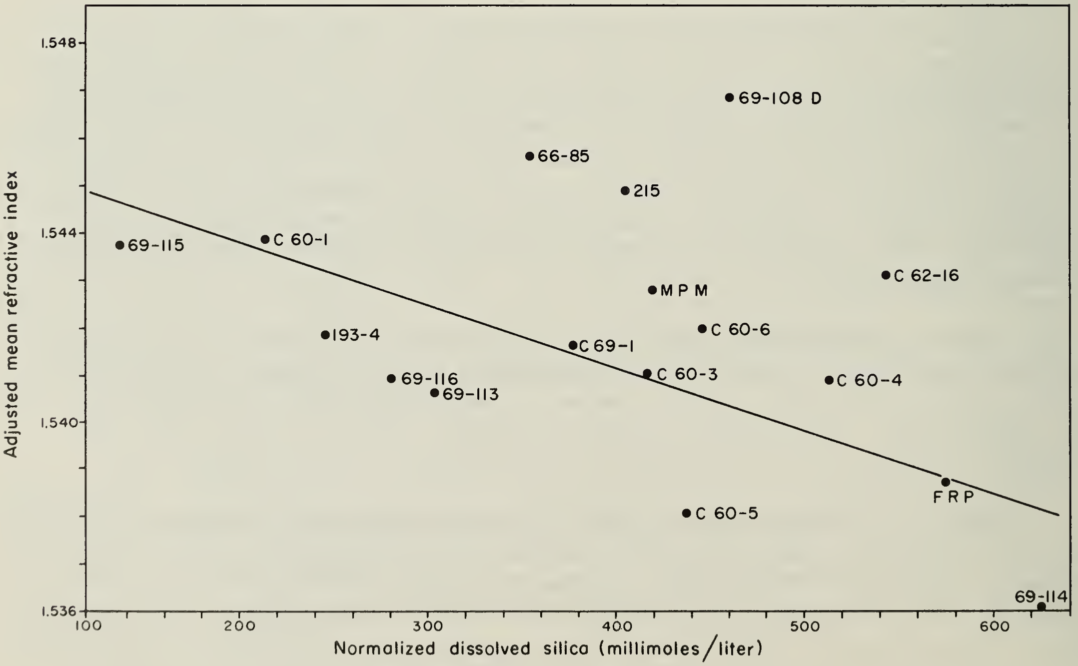

Fig. 6 - Plot of normalized dissolved silica as a function of adjusted mean refractive index.

not lie on the trend of the final graph relating normalized R_C to the adjusted mean refractive index.

In like manner, points falling only on the trend established by the first normalization process were interpreted as representing samples in which the crystallinity of the sample, as defined by the adjusted mean refractive index, played a secondary role in determining the amount of R_C.

The second group of nonconforming points consists of two points that fall along neither trend. These data are from samples that had surface areas more than twice the average for all samples. We postulated that only in this group does the BET surface area play an important role in determining the degree of R_C.

Correlation of the independent variables with S_C values was calculated in the same manner. S_C was plotted as a function of the adjusted mean refractive index (fig. 2). The regression line was shifted along the x-axis until a datum point was intersected. This point was projected along the curve until the line representing the refractive index of quartz, averaged between ϵ and ω indices (1.5485), was intersected. The indicated value at this point of intersection represented the quantity of S_C normalized to the amount the sample would have produced had it been composed of well crystallized quartz.

The normalized S_C plotted against the normative quartz also shows a linear trend (fig. 5). Again, these graphs were interpreted to indicate that the adjusted crystallinity as measured by the mean refractive index was the most important factor influencing the amount of silica going into solution for those samples with datum points falling along the trend. The order of the projection was reversed, and those points not falling along the trend established by the first set of projections did correlate well with the second trend, and vice versa (fig. 6). Only one datum point failed to follow suit, and its surface area was found to be three times higher than the average.

Three other samples had BET surface areas at least twice the average of all samples. These samples, however, tended to follow the general pattern outlined above because they had other properties that tended to counteract the large surface areas. Two samples showed a high degree of crystallinity, and the other sample was composed of a very small amount of normative quartz.

SUMMARY AND CONCLUSIONS

The properties of chert that significantly affect its reduction of alkalinity and dissolved silica—the measured results of the ASTM test—vary from one sample to another. Any one of various properties of chert may be dominant in any given sample and so affect the reactivity of the chert in an alkaline environment.

The crystallinity, as measured by its adjusted mean refractive index, is generally the major determinant of the amount of dissolved silica. Where the percentage of quartz is especially high, however, it may be the prime factor determining the amount of dissolved silica. On the other hand, if the surface area is particularly great (more than 2.00 m^2/g), the effects of crystallinity and of the amount of quartz present may be altered considerably.

In most samples the percentage of normative quartz and the adjusted mean refractive index have nearly equal influence on the degree of reduction in alkalinity in our tests. In a few samples, however, one of these properties may dominate the other. A decrease in the amount of quartz will tend to decrease the reduction, as will an increase in the degree of crystallinity. Where the decrease in quartz content is accompanied by an increase in carbonate content, however, the reduction in alkalinity will not be immediately apparent because of the formation of calcium hydroxide.

The effect of the carbonate may decrease when the chert particles are larger than the individual carbonate grains. Electron microscopy indicates relatively impervious chert frequently surrounds rhombic carbonate grains. Although these carbonate grains contribute to the carbonate content of the whole sample, many would not be available for reaction.

Our study indicates that while ASTM test C 289 may be of value in determining the potential reactivity of chert in concrete, the results of the test must be interpreted with care. The presence of carbonate may influence the test results without having any effect on the behavior of the chert as aggregate. In addition, there appears to be no single property of chert that can be used to predict its reaction in the test, nor is there any combination of properties of the chert that act in a consistent manner in determining its reactivity.

Acknowledgments

Richard C. Mielenz of Master Builders, Cleveland, Ohio, made valuable suggestions that, in large measure, were incorporated into the paper. Clyde E. Kesler of the Civil Engineering Department, University of Illinois, Urbana, read the manuscript and also made helpful suggestions. Certain samples of chert used in this study were obtained from Norman C. Hester, Hermann W. Pfefferkorn, and Bruce Brown of the Illinois State Geological Survey.

REFERENCES

American Society for Testing and Materials, 1970, Standard method of test for potential reactivity of aggregates (chemical method) ASTM Designation C 289-66, in 1970 Annual Book of ASTM Standards, Part 10, Concrete and mineral aggregates: Am. Soc. Testing and Materials, Philadelphia, p. 191.

Azároff, L. V., and M. J. Buerger, 1958, The powder method in X-ray crystallography: McGraw-Hill Book Company, Inc., New York, 342 p.

Buck, A. P., 1961, A study of chert popouts, Wolf River floodwall, Memphis, Tennessee; initial observations: U. S. Army Engr. Waterways Expt. Sta. Technol. Rept. no. 6-581.

Dunn, J. R., and M. A. Ozol, 1962, Deleterious properties of chert: New York State Dept. Public Works, Eng. Research Ser. RR 62-7, 78 p.

Folk, R. L., 1965, Petrology of sedimentary rocks: Hemphill's, Austin, Texas, 159 p.

Folk, R. L., and C. E. Weaver, 1952, A study of the texture and composition of chert: Am. Jour. Science, v. 250, no. 7, p. 498-510.

Frondel, Clifford, 1962, Dana's system of mineralogy; volume III, Silica minerals: John Wiley and Sons, Inc., New York, 334 p.

Gross, K. A., and M. S. Paterson, 1965, Natural X-ray line broadening in limestones and marbles: Am. Jour. Science, v. 263, p. 238-244.

Klassen-Neklyudova, M. V., 1964, Mechanical twinning of crystals [translated]: Consultants Bur., New York, 213 p.

Mather, Kathryn, 1958, Cement-aggregate reaction—What is the problem?, in Trask, P. D. (ed.), Engineering geology case histories no. 2: Geol. Soc. America, p. 17-19.

Michaels, E. L., M. E. Volin, and A. P. Ruotsala, 1964, The properties of chert aggregates in relation to their deleterious effect in concrete: Inst. Mineral Research, Michigan Tech. Univ., Houghton, Rept. 0255, 163 p.

Mielenz, R. C., 1954, Petrographic examination of concrete aggregate: Am. Soc. Testing Materials Proc., v. 54, p. 1188-1218.

Mielenz, R. C., 1958a, Chemical tests for alkali reactivity of concrete aggregate: Highway Research Board Research Rept. 18-C, p. 26-29.

Mielenz, R. C., 1958b, Petrographic examination of concrete aggregate to determine potential alkali reactivity: Highway Research Board Research Rept. 18-C, p. 29-35.

Mielenz, R. C., and E. J. Benton, 1958, Evaluation of the quick chemical test for alkali reactivity of concrete aggregate, in Alkali-aggregate reaction: Highway Research Board Bull. 171, p. 1-15, Natl. Acad Science—Natl. Research Council.

Mielenz, R. C., K. T. Greene, and E. J. Benton, 1947, Chemical test for reactivity of aggregates with cement alkalies; chemical processes in cement-aggregate reaction: Am. Concrete Inst. Jour., v. 44, p. 193-218.

Pelto, C. R., 1956, A study of chalcedony: Am. Jour. Science, v. 254, no. 1, p. 32-50.

Stanton, T. E., 1942, Expansion of concrete through reaction between cement and aggregate: Am. Soc. Chem. Engrs. Trans., v. 107, p. 54-84.

Thomas, Josephus, Jr., and R. R. Frost (in press), Versatile apparatus for studying reactions involving gas adsorption or evolution: Ill. Acad. Sci. Trans.

Wuerpel, C. E., and E. P. Rexford, 1940, The soundness of chert as measured by bulk specific gravity and absorption: Am. Soc. Testing Materials Proc., v. 40, p. 1021.

ILLINOIS STATE GEOLOGICAL SURVEY

Urbana, Illinois 61801

FULL TIME STAFF
February 15, 1972

JOHN C. FRYE, Ph.D., D.Sc., Chief
Hubert E. Risser, Ph.D., Assistant Chief (on leave)

G. R. Eadie, M.S., E.M., Administrative Engineer
Velda A. Millard, Fiscal Assistant to the Chief
Helen E. McMorris, Secretary to the Chief

GEOLOGICAL GROUP

Jack A. Simon, M.S., Principal Geologist
M. L. Thompson, Ph.D., Principal Research Geologist (on leave)
R. E. Bergstrom, Ph.D., Coordinator, Environmental Geology
Frances H. Alsterlund, A.B., Research Associate

COAL

M. E. Hopkins, Ph.D., Geologist and Head
Harold J. Gluskoter, Ph.D., Geologist
William H. Smith, M.S., Geologist
Neely H. Bostick, Ph.D., Associate Geologist
Kenneth E. Clegg, M.S., Associate Geologist
Heinz H. Damberger, D.Sc., Associate Geologist
Russel A. Peppers, Ph.D., Associate Geologist
Roger B. Nance, M.S., Assistant Geologist
George J. Allgaier, B.A., Jr. Assistant Geologist
Kenneth R. Cope, B.S., Research Assistant
Christine M. Pischl, B.S., Research Assistant

OIL AND GAS

Donald C. Bond, Ph.D., Head
Lindell H. Van Dyke, M.S., Geologist
Hubert M. Bristol, M.S., Associate Geologist
Thomas F. Lawry, B.S., Associate Petroleum Engineer
R. F. Mast, M.S., Associate Petroleum Engineer
Wayne F. Meents, Associate Geological Engineer
David L. Stevenson, M.S., Associate Geologist
Richard H. Howard, M.S., Assistant Geologist
Jacob Van Den Berg, M.S., Assistant Geologist
Nancy J. Harper, Technical Assistant
Marjorie E. Melton, Technical Assistant

ENGINEERING GEOLOGY AND TOPOGRAPHIC MAPPING

W. Calhoun Smith, Ph.D., Geologist in charge
Paul B. DuMontelle, M.S., Associate Geologist

CLAY RESOURCES AND CLAY MINERAL TECHNOLOGY

W. Arthur White, Ph.D., Geologist and Head
Bruce F. Bohor, Ph.D., Associate Geologist
Cheryl W. Adkisson, B.S., Research Assistant
Barbara E. Peterson, B.S., Technical Assistant

GEOLOGICAL RECORDS

Vivian Gordon, Head
Hannah Kistler, Supervisory Assistant
Diane L. Heath, B.A., Research Assistant
Elizabeth A. Anderson, Technical Assistant
Betty C. Cox, Technical Assistant
Joann L. Graves, Technical Assistant
Coradel R. Little, A.B., Technical Assistant
Connie L. Maske, B.A., Technical Assistant
Elizabeth Speer, Technical Assistant

GROUND-WATER GEOLOGY AND GEOPHYSICAL EXPLORATION

Robert E. Bergstrom, Ph.D., Geologist and Head
Merlyn B. Buhle, M.S., Geologist
John P. Kempton, Ph.D., Geologist
Keros Cartwright, M.S., Associate Geologist
George M. Hughes, Ph.D., Associate Geologist
Leon R. Follmer, Ph.D., Assistant Geologist
Manoutchehr Heidari, Ph.D., Assistant Engineer
Paul C. Heigold, Ph.D., Assistant Geophysicist
Kemal Piskin, M.S., Assistant Geologist
Philip C. Reed, A.B., Assistant Geologist
Frank B. Sherman, Jr., M.S., Assistant Geologist
Ross D. Brower, M.S., Jr. Assistant Geologist
Jean I. Larsen, M.A., Jr. Assistant Geologist
Joan E. Buehler, A.M., Research Assistant
George P. Zielinski, Technical Assistant

STRATIGRAPHY AND AREAL GEOLOGY

Charles Collinson, Ph.D., Geologist and Head
Elwood Atherton, Ph.D., Geologist
T. C. Buschbach, Ph.D., Geologist
Herbert D. Glass, Ph.D., Geologist
Lois S. Kent, Ph.D., Associate Geologist
Jerry A. Lineback, Ph.D., Associate Geologist
David L. Gross, Ph.D., Assistant Geologist
Alan M. Jacobs, Ph.D., Assistant Geologist
Michael L. Sargent, M.S., Assistant Geologist
Matthew J. Avcin, M.S., Research Assistant
Julia C. Badal, B.S., Research Assistant
James E. Rogers, M.S., Research Assistant
Margaret L. Whaley, B.S., Research Assistant
Mildred R. Newhouse, Technical Assistant

INDUSTRIAL MINERALS

James C. Bradbury, Ph.D., Geologist and Head
James W. Baxter, Ph.D., Geologist
Richard D. Harvey, Ph.D., Geologist
Norman C. Hester, Ph.D., Assistant Geologist
George M. Wilson, M.S., Assistant Geologist

GEOLOGICAL SAMPLES LIBRARY

Robert W. Frame, Superintendent
J. Stanton Bonwell, Supervisory Assistant
Charles J. Zelinsky, Supervisory Assistant
Eugene W. Meier, Technical Assistant

CHEMICAL GROUP

Glenn C. Finger, Ph.D., Principal Chemist
G. Robert Yohe, Ph.D., Senior Chemist
Thelma J. Chapman, B.A., Research Assistant
N. F. Shimp, Ph.D., Coordinator, Environmental Research
Anita E. Bergman, B.S., Technical Assistant

MINERALS ENGINEERING

R. J. Helfinstine, M.S., Mechanical Engineer and Head
H. P. Ehrlinger III, M.S., E.M., Assoc. Minerals Engineer
John M. Masters, M.S., Assistant Mineralogist
Lee D. Arnold, B.S., Research Assistant
Walter E. Cooper, Technical Associate
Robert M. Fairfield, Supervisory Assistant
Jimmie D. Cooper, Technical Assistant
John P. McClellan, Technical Assistant (on leave)
Edward A. Schaede, Technical Assistant (on leave)

GEOCHEMISTRY

G. C. Finger, Ph.D., Acting Head
Donald R. Dickerson, Ph.D., Organic Chemist
Josephus Thomas, Jr., Ph.D., Physical Chemist
Richard H. Shiley, M.S., Associate Organic Chemist
Robert R. Frost, Ph.D., Assistant Physical Chemist
Ralph S. Boswell, Technical Assistant

(Chemical Group continued on next page)

CHEMICAL GROUP — Continued

ANALYTICAL CHEMISTRY

Neil F. Shimp, Ph.D., Chemist and Head
Rodney R. Ruch, Ph.D., Chemist
William J. Armon, M.S., Associate Chemist
John A. Schleicher, B.S., Associate Chemist
Larry R. Camp, B.S., Assistant Chemist
Dennis D. Coleman, M.S., Assistant Chemist
David B. Heck, B.S., Assistant Chemist
L. R. Henderson, B.S., Assistant Chemist
F. E. Joyce Frost, Ph.D., Assistant Chemist
Lawrence B. Kohlenberger, B.S., Assistant Chemist
John K. Kuhn, B.S., Assistant Chemist
Patricia M. Santoliquido, S.B., Special Research Associate
William C. Harfst, B.S., Special Research Assistant
Joan D. Hauri, B.A., Special Research Assistant
Paul E. Gardner, Technical Assistant
George R. James, Technical Assistant

MINERAL ECONOMICS GROUP

Hubert E. Risser, Ph.D., Principal Mineral Economist (on leave)
W. L. Busch, A.B., Economic Analyst
Robert L. Major, M.S., Assistant Mineral Economist
Irma E. Samson, Clerk Typist II

ADMINISTRATIVE GROUP

George R. Eadie, M.S., E.M., Head
Paula A. Manny, B.S., Research Assistant

TECHNICAL RECORDS

Miriam Hatch, Supervisor
Carol E. Fiock, Technical Assistant
Hester L. Nesmith, B.S., Technical Assistant

PUBLICATIONS

Betty M. Lynch, B.Ed., Technical Editor
Mary Ann Noonan, A.M., Technical Editor
Jane E. Busey, B.S., Assistant Technical Editor
Dorothy Rae Weldon, Editorial Assistant
Marie L. Martin, Geologic Draftsman
Ilona Sandorfi, Assistant Geologic Draftsman
Patricia A. Whelan, B.F.A., Asst. Geologic Draftsman
William Dale Farris, Scientific Photographer
Dorothy H. Huffman, Technical Assistant

GENERAL SCIENTIFIC INFORMATION

Peggy H. Schroeder, B.A., Research Assistant
Florence J. Partenheimer, Technical Assistant

SPECIAL TECHNICAL SERVICES

Ernest R. Adair, Technical Assistant
David B. Cooley, Administrative Assistant
Wayne W. Nofftz, Distributions Supervisor
Glenn G. Poor, Research Associate (on leave)
Merle Ridgley, Instrument Specialist
James E. Taylor, Automotive Mechanic
Donovon M. Watkins, Technical Assistant

FINANCIAL OFFICE

Velda A. Millard, in charge
Marjorie J. Hatch, Account Technician I
Pauline Mitchell, Account Technician I
Virginia C. Smith, B.S., Account Technician I

CLERICAL SERVICES

Nancy J. Hansen, Secretary I
Hazel V. Orr, Clerk-Stenographer III
Mary K. Rosalius, Clerk-Stenographer II
Lucy Wagner, Clerk-Stenographer II
Francie W. Doll, Clerk-Stenographer I
Janette L. Hall, Clerk-Stenographer I
Theresa J. Martin, Clerk-Stenographer I
Edna M. Yeargin, Clerk-Stenographer I
JoAnn L. Lynch, Clerk-Typist II
Judith Ann Muse, Clerk-Typist II
Pauline F. Tate, Clerk-Typist II

EDUCATIONAL EXTENSION

David L. Reinertsen, A.M., Geologist and Acting Head
Dwain J. Berggren, M.A., Jr. Assistant Geologist
Myrna M. Killey, B.A., Research Assistant

LIBRARY

Mary P. Krick, M.S., Geological Librarian
Linda K. Clem, B.S., Assistant Librarian

EMERITI

J. S. Machin, Ph.D., Principal Chemist
O. W. Rees, Ph.D., Principal Research Chemist
W. H. Voskuil, Ph.D., Principal Mineral Economist
A. H. Bell, Ph.D., Geologist
George E. Ekblaw, Ph.D., Geologist
H. W. Jackman, M.S.E., Chemical Engineer
J. E. Lamar, B.S., Geologist
L. D. McVicker, B.S., Chemist
Enid Townley, M.S., Geologist
Lester L. Whiting, M.S., Geologist
H. B. Willman, Ph.D., Geologist
Juanita Witters, M.S., Physicist

RESEARCH AFFILIATES AND CONSULTANTS

Richard C. Anderson, Ph.D., Augustana College
W. F. Bradley, Ph.D., University of Texas
David A. Castillon, M.A., Lincoln College
John P. Ford, Ph.D., Eastern Illinois University
Donald L. Graf, Ph.D., University of Illinois
S. E. Harris, Jr., Ph.D., Southern Illinois University
W. Hilton Johnson, Ph.D., University of Illinois
Harry V. Leland, Ph.D., University of Illinois
A. Byron Leonard, Ph.D., University of Kansas
Lyle D. McGinnis, Ph.D., Northern Illinois University
I. Edgar Odom, Ph.D., Northern Illinois University
T. K. Searight, Ph.D., Illinois State University
George W. White, Ph.D., University of Illinois

Topographic mapping in cooperation with the
United States Geological Survey.

Illinois State Geological Survey Circular 468
31 p., 2 pls., 6 figs., 2500 cop., 1972
Urbana, Illinois 61801

Printed by Authority of State of Illinois, Ch. 127, IRS, Par. 58.25.
E 1-11-0

CIRCULAR 468

ILLINOIS STATE GEOLOGICAL SURVEY

URBANA, IL 61801